

Differential absorption spectrometer for pulsed bremsstrahlung

Steven G. Gorbics and N. R. Pereira

Berkeley Research Associates, P.O. Box 852, Springfield, Virginia 22150

(Received 23 March 1992; accepted for publication 10 March 1993)

We describe a differential absorption spectrometer that measures the energy spectrum (from 20 to 800 keV) of flash x rays whose intensity precludes pulse-height analysis methods. The spectrometer uses individually calibrated thermoluminescent dosimeters, each inside its own spherical absorber, to accommodate isotropic radiation from pulsed bremsstrahlung sources. An iterative perturbation unfolding code determines the spectrum from the detector responses and the computed energy response functions. Unfolding works best with a good guess for the initial spectrum, and data with less than a few percent error.

I. INTRODUCTION

The energy spectrum of the x rays from flash x-ray generators can be determined conveniently by unfolding the responses of dose detectors behind x-ray filters of various materials with different thicknesses. A common geometry is to place the detectors in a stack, with filters in between. However, for isotropic x-ray sources that are large compared to the detector stack a straight stack becomes sensitive to the direction of the x rays. However, placing each detector in its own spherical shell that acts as the x-ray filter makes the instrument insensitive to the x-ray direction. Our version of such an instrument has been used to determine the time-integrated x-ray spectrum on various¹⁻⁴ large flash x-ray machines without having given a full account of the measurement technique. The purpose of this paper is to provide a more complete description of the instrument and of the unfolding technique.

The spectrometer's energy regime is from tens of keV to just under 1 MV, perhaps up to 600–800 keV. The upper limit is common to all differential filtering techniques. The Time-Projection Compton Spectrometer,⁵ which uses the energy spectrum of Compton electrons, is able to go beyond 1 MeV at a considerable expense in complexity while giving up the possibility for time resolution of the spectrum. However, replacing the dose detectors by dose rate detectors would yield a time-resolved energy spectrum.

Unfolding of filtered data to determine spectra is used in many other fields, e.g., neutron spectroscopy, and some of the unfolding algorithms have first been developed there. Various of the better-known algorithms invert matrices subject to certain constraints, but our unfolding approach is a simple iterative method that is quite convenient and works very well. It is discussed after the description of the instrument.

II. INSTRUMENTATION

The spectrometer consists of 13 spherical absorption shells configured on a 16.5 cm ($6\frac{1}{2}$ in.) diam circle. The shells' thicknesses range from 0.159 ($\frac{1}{6}$ in.) to 1.27 cm ($\frac{1}{2}$ in.). Inside the shell is a 0.953 cm ($\frac{3}{8}$ in.) diam cavity that contains the detector, a $\text{CaF}_2:\text{Mn}$ thermoluminescent dosimeter (TLD) wrapped in a single layer of 0.0025 cm (1 mil) thick aluminum foil.

The shells are made from aluminum, titanium, copper, and a material with high density and atomic number. Suitable materials are depleted uranium or tungsten. (Lead is of a lower density and is too soft.) Each sphere has a characteristic cutoff below which the response of the enclosed TLD becomes negligible. Table I gives the parameters for each sphere, and the approximate energy at which the response falls to one-tenth of the maximum for each. The thickness and materials of the shells are chosen to give response functions that are spread more or less uniformly on a logarithmic scale over the range of x-ray energies to be measured.

The spectrometer is an improvement over earlier differentially filtered dose measuring techniques in several aspects. The thermoluminescent detectors (Harshaw Chemical Company TLD-400) can be calibrated to a precision of about 1.5%. This high precision facilitates the spectral unfolding process and removes the need for the large number of detectors necessary in previous absorption spectrometers. The excellent sensitivity and wide dose range of the detectors allows measurements in radiation fields of widely varying intensity.

Placing each individual TLD in its own spherical shell reduces the directionality of the instrument. This feature is especially useful in measuring the largely isotropic x-ray fields produced by the typical flash x-ray generator. Individual spheres also add a degree of versatility. The set of spheres in Table I is not unique and can be altered as needed. For example, to measure the spectrum of a 300 keV x-ray generator, the three depleted uranium spheres and the largest copper sphere can be left out of the system. Thus the spectrometer fits in a physically smaller space. It is also possible to improve the resolution in a given energy region by adding additional spheres whose response functions have energy cutoffs in the desired range.

The low-level radioactivity of the depleted uranium exposes the enclosed detectors to ≈ 400 mrad/h. For high-dose applications where the dose per shot behind the uranium is up to 100 rad the small background exposure is no problem, but for applications with around 1 rad per shot the TLDs cannot be left inside longer than a few minutes, which is inconvenient. Present versions of the spectrometer have replaced the depleted uranium with tungsten, so that the TLDs can be left inside the spheres for arbitrarily long

TABLE I. Spectrometer configuration.

Absorber material	Detector No.	Thickness (cm)	Cutoff (MeV)
Aluminum	1	0.159	0.015
	2	0.318	0.020
	3	0.635	0.022
	4	0.953	0.028
Titanium	5	0.159	0.030
	6	0.318	0.034
	7	0.635	0.043
Copper	8	0.318	0.055
	9	0.635	0.070
	10	1.19	0.105
Uranium	11	0.159	0.230
	12	0.318	0.315
	13	0.635	0.410
(in a more recent configuration without uranium)			
Tungsten	11	0.159	0.205
	12	0.318	0.250
	13	0.635	0.310

times. Using tungsten gives only a slight loss in the high-energy capability, e.g., a cutoff energy of 0.31 MeV for tungsten compared to 0.41 MeV for uranium.

The way in which the spheres are arranged in the spectrometer is not critical since the cross-talk between individual elements is minimal. For calibrations the spheres are placed on the perimeter of a 16.5 cm diam circle. When space is limited the spheres can be placed within a 10 cm circle. For measurements in static fields or in pulsed environments where the shot-to-shot reproducibility is good, the spheres can be irradiated individually, reducing the space requirements even further. An additional advantage is the simple mechanical design, which allows users to build their own system at low cost.

The upper energy limit of the spectrometer, about 0.8 MeV, is a disadvantage that is common to all differential absorption spectrometers. Even in the highest atomic number materials the energy absorption for high-energy x rays does not vary sufficiently to give response functions that differ enough to unfold the spectrum. Spectral information for the higher energies can be obtained by other methods such as Compton spectroscopy and photoactivation. The usefulness at low energies depends on the amount of energy in the spectrum above the region of interest. Typically, the lower energy limit for bremsstrahlung with end points of the order of 1 MeV is ≈ 10 –20 keV. All detectors are sensitive to high-energy x rays. Therefore, when a large part of the dose is from photons around 1 MeV the differences between the individual detector responses are reduced. In addition, the fit in the higher-energy portion of the spectrum becomes dependent upon the form of the starting spectrum.

Another disadvantage is the high precision of the detectors needed for acceptable unfolding of the spectra with a limited number of detectors. To achieve the 1.5% precision in the detectors, it is necessary to calibrate the TLD chips individually. The chips are normally read the day

after the irradiation to minimize the effects of fading of the signal, reannealed, and exposed to a Co^{60} calibration dose. The calibration dose is then read 24 h later and each reading is corrected for the individual sensitivity of the chip. The time needed for this sequence can be reduced to a few hours but the procedure is laborious and results in an appreciable time delay in the spectral determination. In cases where the accuracy in the spectral unfold is not a primary requirement the $\approx 5\%$ precision of batch-calibrated dosimeters may be sufficient.

The relatively large size of the spectrometer package is a minor disadvantage. The smallest configuration of the spheres is still a 10 cm circle and, in some applications, the field is not spatially uniform over that area. Fortunately, the high sensitivity of the detectors can often solve this problem by allowing the spectrometer to be placed farther away from the source, at a position where the field has become sufficiently uniform.

III. THE UNFOLDING PROCESS

An accurate and consistent set of energy response functions is critical to the quality of the measurement. The responses can be approximated using the known attenuation coefficients, computed with an electron-photon transport code such as ITS,⁶ and the results can be compared to measurements with a known spectrum. In the computations, done with the ITS member code ACCEPT that allows three spatial dimensions, a unidirectional and monoenergetic photon beam impinges on each of the spheres. The beam is 0.6 cm in radius, slightly larger than the cavity but smaller than the sphere itself. The flat face of the TLD is perpendicular to the beam and fills the cavity to within 0.05 mm of the edge. The remainder of the cavity is filled with nitrogen to allow electron transport from the shielding to the TLD, but the 1 mil aluminum foil is omitted. The computational geometry deviates from the experimental geometry for computational efficiency only. Increasing the beam size or decreasing the TLD size has no detectable effect on the response function when checked for a few energies and spheres (to within the statistical accuracy of $\approx 2\%$ for the vast majority of the data.)

The response functions are shown in Fig. 1. The calculated functions compare favorably with measurements made at Co^{60} and Cs^{137} energies, as well as with a series of heavily filtered spectra from a 300 keV x-ray generator.

An integral part of any differential technique is the unfolding procedure needed to obtain the unknown spectrum. Many unfolding algorithms use matrix inversion.⁷ Our spectrometer uses an iterative perturbation method developed for the determination of neutron spectra from Bonner sphere data.^{8,9} This algorithm facilitates the determination of an appropriate¹⁰ spectrum by a convenient imposition of constraints on the solution, such as varying degrees of smoothing, prohibition of negative values, and the choice of a proper best-guess input spectrum. Further comparisons between the merits of the different unfolding techniques are not appropriate here except to mention that our choice of an iterative method is partly historical, and

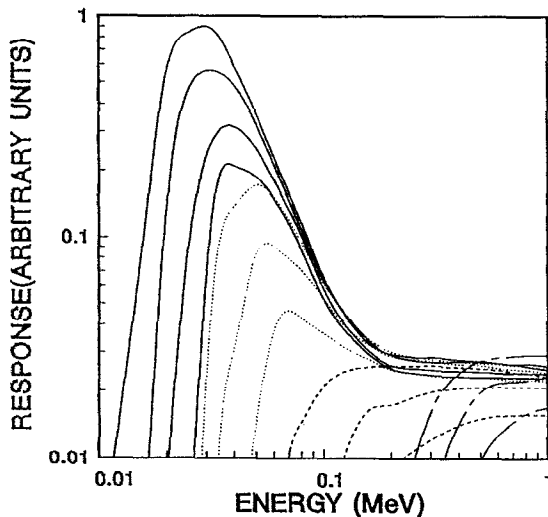


FIG. 1. Detector response functions. The solid lines correspond to the four aluminum absorption shells, the dotted lines to the three titanium shells, the three dashed lines to the copper absorption shells, and the chain-dashed line to the three tungsten shells. For the shell thicknesses see Table I.

does not imply that alternatives might not be equally (or even more) useful.

The response Q_i of the i th detector is given by

$$Q_i = \int d(h\nu) R_i(h\nu) S(h\nu),$$

where $S(h\nu)$ is the x-ray spectrum to be determined and $R_i(h\nu)$ is the energy response function for each detector. This equation is discretized to j energy bins, $(h\nu)_j$, to give

$$Q_i = \sum_j R_i(h\nu)_j S(h\nu)_j \Delta(h\nu)_j,$$

i.e., the solution of i equations in j unknowns for the spectral values $S(h\nu)_j$ that best fit the detector readings Q_i given the response functions $R_i(h\nu)_j$.

It is possible to choose the number of energy bins equal to the number of detectors. However, choosing an underdetermined system, more energy bins than detector response values, allows the above-mentioned constraints to be easily imposed on the solution. On physical grounds the spectrum must be continuous, except perhaps for the k line of the bremsstrahlung converter's material. This k line may give a peak in a specific energy bin below 0.1 MeV that can be included in the input spectrum. At the higher energies the shape of the theoretical bremsstrahlung spectrum can be used as a guide.

The spectrometer has 13 detectors and the unfolding procedure uses 10 energy bins per decade, centered on the even decade energies. The choice of the number of energy bins is purely arbitrary. In this case the number is large enough to ensure an underdetermined set of equations, and small enough to keep the computing time within reasonable limits. The code YOGI finds the spectrum by starting from some initial spectrum and computing a set of detector responses Q_i . These are compared with the measured values to determine an error parameter, here the mean square

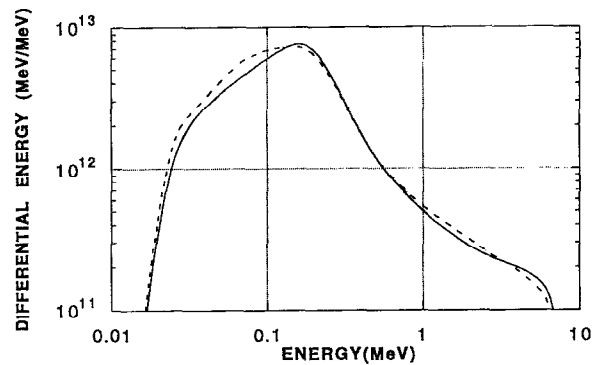


FIG. 2. The spectrum unfolded from the identical experimental data with different response functions. Solid line: spectrum (see Ref. 4) using density of pure tungsten. Dashed line: spectrum recomputed with actual density of tungsten alloy used in tungsten spheres.

deviation. The code then perturbs one point in the trial spectrum by a fixed amount and recalculates the error. The old point is kept if the error gets worse, but if the error improves the new point is substituted. The amount of an individual perturbation can be determined when the fit is done but normally is between 0.1% and 1%. This procedure is repeated for randomly chosen spectrum points until a fixed number of perturbations have been done or the error remains below some tolerance level.

YOGI works very well. Choosing a reasonable trial spectrum helps: for bremsstrahlung a filtered Kramers spectrum is appropriate. More importantly, it is necessary to impose a degree of "smoothness" as an auxiliary condition. Smoothing is done by adjusting the points on either side of the perturbed point by a fixed fraction of the change. A 10% adjustment results in a moderate amount of smoothing on the final curve.

IV. ESTIMATE OF ERRORS

The uncertainties in spectra produced by this kind of unfolding process come from several separate sources. A basic problem is the accuracy of the detector response as a function of energy. Even a perfect unfolding of the data results in an erroneous spectrum if the response functions do not correspond to reality.

Figure 2 shows the spectrum measured in the backscatter geometry on the Aurora flash x-ray generator. The solid line is the spectrum determined at the time of the experiment.⁴ The dashed line is the spectrum inferred from the same experimental data with recomputed response functions. The modification reflects the difference between the density of pure tungsten (19.3 g/cm^3) as compared to the actual density (17.8 g/cm^3) of the machinable copper-tungsten alloy used in the spheres. The spectra are very close, but still visibly different.

A second source of error is the capability of the unfolding code. Given an accurate response function but data with random errors with known error bars, how well can the program unfold these values to produce a spectrum?

The amount of error in the calculated spectrum depends on several conditions.

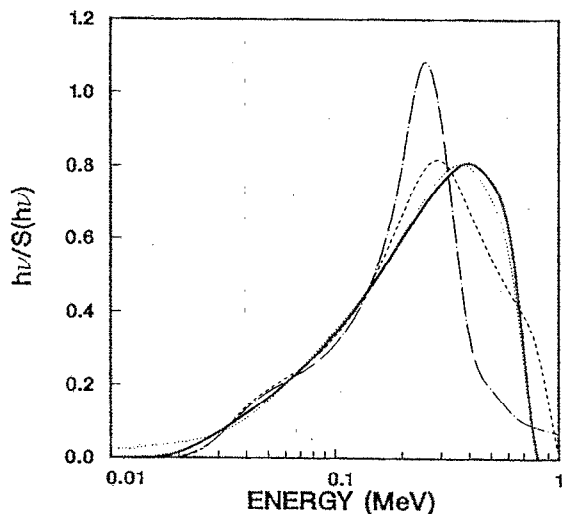


FIG. 3. The effect of different starting spectra on the unfolded spectrum. The solid curve is the original spectrum (800 keV end point with 1.0 g/cm^2 Al absorption); the chain-dot curve was produced from a flat starting spectrum; the dotted curve has the proper high-energy cutoff added; and the dashed curve is produced from a reasonable but wrong guess for a starting spectrum (1 MeV end point with 0.5 g/cm^2 Al absorption).

(1) Any lack of precision of the individual detectors is an obvious source of error. The unfolding procedure depends on differences between detector responses. The accuracy of differences can be much worse than that of the responses themselves, and these larger inaccuracies work through in the spectrum.

(2) Are the absorbers selected suitable for the energy range of interest? An optimum set of absorbers may examine only a specific portion of the energy spectrum.

(3) It is difficult to unfold the data in the lower portion of a spectrum when an appreciable fraction of the total energy is above that region. Each detector responds to all energies above some lower limit. If a large fraction of the dose comes from the higher energies, the spectrum must be found from small differences between large numbers.

(4) In addition, unfolding is inaccurate for energies above a few hundred keV. The problem in this region is intrinsic to absorption spectrometers.

The influence of the different error sources can be investigated empirically. Suitable test spectra are the Kramers bremsstrahlung spectra, with different end-point energies and attenuated by a typical converter package. As an example, a spectrum with a 0.8 MeV end point, attenuated with 1.0 g/cm^2 of aluminum is used. The detector responses for each of the detectors are computed from the individual response functions and this spectrum. YOGI is then called upon to get back the spectrum.

Figure 3 illustrates the effect of the trial spectrum that is input to the code. The axes in this and the subsequent figures are chosen such that the area under the curve is proportional to the fluence. The unfolded spectra are shown without any additional normalizations either in energy or intensity.

Figure 3 shows the final fit on the spectrum when the initial input spectrum is flat (chain dot), flat with only the

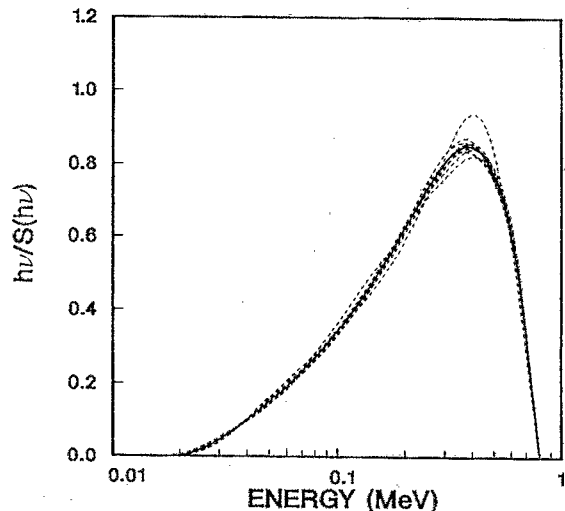


FIG. 4. Energy spectra unfolded from detector responses with superposed random errors of 1% (dashed lines). The solid line is the initial spectrum.

high-energy cutoff included (dot), and a Kramers spectrum with a higher end point (1.0 MeV) and a lesser amount of attenuation (0.5 g/cm^2). The solid curve in the figure is the original spectrum. It must be emphasized that each spectrum in the figure fits the input data equally well. The shape of the high-energy portion of the spectrum depends strongly on the right guess for the energy end point, a quantity that normally is known from the machine parameters.

Having established YOGI's capability to find the initial spectrum from ideal data, it is important to determine the sensitivity of the spectrum to realistic detector responses. Besides systematic errors, the detector responses contain random errors. These experimental errors are often^{11,12} mimicked by adulterating the ideal responses with various amounts of statistically random errors. Spectral unfolding then gives a range of possible spectra. The vari-

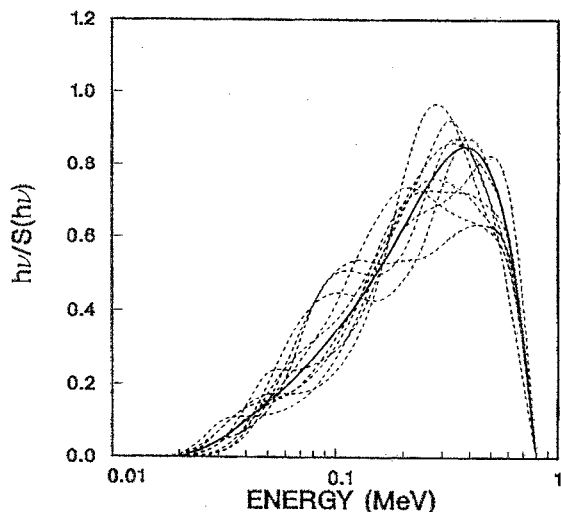


FIG. 5. Energy spectra unfolded from detector responses with superposed random errors of 10% (dashed lines). The solid line is the initial spectrum.

TABLE II. Error propagation-energy bins.

E_{max} (keV)	TLD Error (%)	Standard deviation (%) in energy bin centered at					
		32 keV	80 keV	100 keV	250 keV	500 keV	1 MeV
400	1	3.18	1.95	1.72	1.31
	5	13.5	6.57	7.15	6.52
	10	17.7	15.51	19.0	18.23
800	1	3.82	2.27	2.26	1.69	1.02	...
	5	12.0	11.0	13.4	9.71	4.57	...
	10	31.1	20.3	27.0	13.6	6.25	...
2000	1	3.60	3.17	2.43	3.00	2.95	1.59
	5	16.8	16.5	16.9	10.4	12.7	5.95
	10	28.8	32.0	30.44	28.0	24.9	13.6

ation of these spectra represents the sensitivity of the spectrum due to imprecision in the dose readings.

Figures 4 and 5 show the results of this procedure. Figure 4 gives the starting spectrum for 0.8 MeV (solid line), and 10 samples of 0.8 MeV end-point spectra when 1% rms noise is added to the detector responses. The 10 spectra determined from the noisy data appear to be acceptably close to the ideal spectrum, and to each other. Table II shows numerically how the error propagates in various energy bins. The error in the spectrum is about thrice the error in the detector responses, except toward the high-energy end of the spectrum, where the errors in the spectrum are comparable to the noise in the input data. This counterintuitive feature comes from the softness of the fit in that region of the spectrum.

Figure 5 shows the 0.8 MeV end-point spectra compared with the spectra unfolded from responses with 10% rms noise added. The accuracy is visibly worse, especially in the middle of the spectral range. Table II gives the numerical values for the errors observed in the different energy bins. The error propagation appears to be linear in the initial error, i.e., a 10% error in the data gives a 30% error in the lower energy bins of the spectrum, reduced to about 10% at the high end.

Table III shows how the errors in the detector responses translate to the fluence and dose (Si). The table shows that the total energy can be determined with an error of about a third of the error of the input data. This reflects the $N=13$ detectors whose responses are independently randomized, resulting in an error reduced by a fac-

tor \sqrt{N} . The dose [rad(Si)] has an error that is roughly equal to the detector error. This is because the dose is dominated by the spectrum below about 100 keV.

V. DISCUSSION

The spectrometer has been used to measure the spectrum of several of the major flash x-ray simulators,¹ including Casino and Phoenix, both at the Naval Surface Warfare Center, Blackjack 5 at Maxwell Laboratories, and Python at Physics International. The spectrometer was essential in the development of Aurora's backscatter mode²⁻⁴ at Harry Diamond Laboratories. The measured spectra agree with the spectra calculated for the simulators.

The unfolded spectrum allows calculation of dose-related quantities such as total dose and depth dose in silicon, or in any other relevant material (e.g., GaAs). These depend on absorption of photons from the whole spectrum, and thus have a higher degree of reliability than the spectrum itself (see Table II).

The spectrometer has proven to be a convenient and useful instrument for time-integrated flash x-ray measurements. Also, the TLDs are being replaced by fast detectors such as plastic scintillators or photoconductive elements. The time-resolved dose rates can then be unfolded to give the radiation spectrum as it varies during the radiation pulse.

ACKNOWLEDGMENTS

We would like to thank the referee and Dr. D. L. Fehl for suggesting additional references.

TABLE III. Error propagation-fluence and dose.

E_{max} (keV)	TLD Error (%)	Standard deviation of fluence (%)	Standard deviation of dose (%)
400	1	0.25	1.10
	5	1.85	4.08
	10	4.66	7.77
800	1	0.37	1.00
	5	1.28	3.47
	10	3.38	8.47
2000	1	0.40	0.91
	5	1.06	3.04
	10	3.50	5.18

¹S. G. Gorbics and N. R. Pereira, J. Radiation Effects, Res. Eng. 1, 57 (1988).

²N. R. Pereira, J. Appl. Phys. 57, 1445 (1984).

³D. A. Whittaker, K. G. Kerris, M. Litz, S. G. Gorbics, and N. R. Pereira, J. Appl. Phys. 58, 1034 (1985).

⁴K. G. Kerris, F. J. Agee, D. A. Whittaker, S. G. Gorbics, and N. R. Pereira, J. Appl. Phys. 65, 5 (1989).

⁵G. T. Baldwin and J. R. Lee, IEEE Trans. Nucl. Sci. NS-33, 1298 (1986); G. T. Baldwin, C. O. Landron, J. R. Lee, and L. J. Lorence, Sandia National Laboratories Report No. SAND89-0448, Albuquerque, NM 1989.

⁶J. A. Halbleib and T. A. Mehlhorn, ITS: The Integrated TIGER Series of Coupled Electron/Photon Monte Carlo Transport Codes, Version

2.1: SAND-0573 1984; J. A. Halbleib, R. P. Kensek, T. A. Mehlhorn, S. M. Seltzer, M. J. Berger, ITS Version 3.0: The Integrated TIGER Series ..., SAND91-1634, March 1992.

⁷For a general discussion of unfolding see I. J. D. Craig and J. C. Brown, *Inverse Problems in Astronomy* (Hilger, Bristol, 1986). Widely used unfolding codes based on matrix methods include STAY'SL (F. G. Perey, ORNL/TM-6062, 1977), and LSL (F. W. Stallman, NUREG/CR-0029, 1983). These codes are available from the Radiation Shielding Information Center, ORNL.

⁸T. L. Johnson and S. G. Gorbics, *Health Phys.* **41**, 859 (1981).

⁹T. L. Johnson, Y. Lee, K. A. Lowry, and S. G. Gorbics, *Proceedings of Theory and Practices in Radiation Protection and Shielding*, American Nuclear Society Topical Conference, Knoxville, TN, 1987 (ANS, Argonne, 1987), Vol. 1, p. 83.

¹⁰For a discussion of "appropriate" see R. Gold, Argonne National Laboratory, Report No. ANL-6982 (1964), in addition to Ref. 2.

¹¹D. G. Shirk and N. M. Hoffman, *Rev. Sci. Instrum.* **56**, 809 (1985).

¹²D. L. Fehl, Proceedings of the 8th IEEE Pulse Power Conference, San Diego, CA, 1991 (unpublished).